

Testing for Asymmetries and Anisotropies in Regional Economic Models

Giuseppe Arbia*, Marco Bee†
Giuseppe Espa‡, Flavio Santi§

15th September 2015

Abstract

This paper develops a new methodology for estimating and testing the form of anisotropy of homogeneous spatial processes. We derive a generalised version of the isotropy test proposed by Arbia, Bee and Espa (2013) and analyse its properties in various settings. In light of this, we derive a new approach that allows one to estimate and test under mild conditions any form of anisotropy in homogeneous spatial processes. The power of the test is studied by means of Monte Carlo simulations performed both on regularly and irregularly spaced data.

1 Introduction

A stochastic spatial process is said to be isotropic whenever it is stationary with respect to rotations of its index set about the origin (Ripley 1981, p. 10).

The assumption of isotropy may lead to inconsistent estimates if it is not borne out by data, similarly to what happens when incorrectly assuming other forms of stationarity. This is the main reason why it should be formally tested before fitting any kind of isotropic model.

Over the last decades, the problem of testing isotropy of stochastic spatial processes has been given more attention than in the past, and isotropy tests have been proposed for stochastic surfaces (Cabaña 1987), point processes (see e.g. Guan, Sherman and Calvin 2004), lattice data (Molina and Feito 2002), and (regularly or irregularly-spaced) areal data (Arbia, Bee and Espa 2013). In this paper we focus on the problem of testing isotropy in models for areal data.

In some cases, it is possible to apply isotropy tests like those of Guan, Sherman and Calvin (2004) or Molina and Feito (2002) to irregularly-spaced areal data, however two features of areal data models may make such adaptations not suitable, especially in econometric analysis.

*Department of Statistics, Catholic University of the Sacred Heart, L.go Francesco Vito 1, 00168 Rome. E-mail: giuseppe.arbia@rm.unicatt.it.

†Department of Economics and Management, University of Trento, Via Inama 5, 38122 Trento. E-mail: marco.bee@unitn.it.

‡Department of Economics and Management, University of Trento, Via Inama 5, 38122 Trento. E-mail: giuseppe.espa@unitn.it.

§Department of Social and Economic Sciences, Sapienza University of Rome, P.le Aldo Moro 5, 00185 Rome. E-mail: flavio.santi@uniroma1.it.

First, the geometric distance between centroids of cells may not be the most suitable criterion for assessing isotropy of a process which has been modelled through a weight matrix. Indeed, most of the times the physical distance has a minor or no role in defining the weight matrix of an econometric spatial model. It follows that, in such cases, an isotropy test based on variograms (like Guan, Sherman and Calvin 2004) or other functions of physical distance may be inconsistent with the modelling approach being adopted.

Second, samples of irregular areal data are often rather small, especially in econometric analysis. This implies that isotropy tests requiring large samples to be applied cannot be used. This is the case, for instance, of the isotropy test proposed by Molina and Feito (2002), which achieves the independence from distance over a rectangular grid by randomly choosing observations from the original sample, and considering just their mutual directions. Although such method can be adapted in order to be suitable also on irregularly-spaced grids, it can provide precise and reliable outcomes only in large samples.

The isotropy test proposed by Arbia, Bee and Espa (hereinafter ABE) has been developed for econometric models, and overcomes both problems just described. The ABE test requires the neighbours of each cell to be split into two groups according to an arbitrary direction, and tests whether the spatial dependence is statistically different between them. The test works well in many cases, but it may fail to detect some forms of anisotropies, as the following example shows.

Example 1. Consider the spatial process $\{y_{st}\}$ defined on a rectangular lattice \mathcal{G}_n :

$$y_{st} = \alpha(y_{s-1,t} + y_{s,t+1}) + \beta(y_{s+1,t} + y_{s,t-1}) + \varepsilon_{st}, \quad (1)$$

where $\alpha \neq \beta$ are parameters, and $\{\varepsilon_{st}\}$ is an iid spatial process. The process (1) is clearly anisotropic (since $\alpha \neq \beta$).

If we observe the process $\{y_{st}\}$, and test for isotropy by means of the ABE test, we may split neighbours along the NW–SE direction, and fit the model:

$$y_{st} = \rho_1(y_{s-1,t} + y_{s,t+1}) + \rho_2(y_{s+1,t} + y_{s,t-1}) + e_{st}. \quad (2)$$

The isotropy assumption is not rejected if ρ_1 and ρ_2 are not statistically different from each other. For this specification of the test, model (2) coincides with the data generating process (1), and it is possible to detect anisotropy provided that the sample size is large enough.

Now assume that we split neighbours along to a different direction. For instance, we may choose the SW–NE direction, and fit the following model:

$$y_{st} = \rho_1(y_{s-1,t} + y_{s,t-1}) + \rho_2(y_{s+1,t} + y_{s,t+1}) + u_{st}. \quad (3)$$

Like (2), also model (3) is consistent with the ABE method, however, if model (3) is fitted, the anisotropy cannot be detected, whatever the sample size is. This happens because each coefficient ρ synthesises the spatial dependence originating from a neighbour with coefficient α and one with coefficient β . \square

Example 1 reveals two problems. First, the ABE test is not rotation-invariant, that is, its outcome depends on the direction chosen for splitting neighbours, which may strongly affect the power of the test, as it will be formally shown hereafter. Second, there may be compensations between coefficients of the

neighbours belonging to the same half-plane, and this may result in a substantial reduction in the power of the test.

In this paper we extend the ABE test to a generic number q of groups of neighbours (this will be called the q -directional ABE test) and provide a formal analysis of the factors affecting its power and of the kind of anisotropies it is able to detect.

In light of this analysis, we propose a new approach that allows one to estimate and test the form of anisotropy of any given spatial process without incurring the problems outlined above. This method leads to a semi-parametric strategy for estimating and testing spatial anisotropy, based on a Fourier expansion of the function that describes the directional dependence. Unlike the q -directional ABE test, this technique does not suffer from multicollinearity problems when a fine estimation of the directional dependence function is required.

This approach is flexible and can be easily adapted and applied to models for areal data like SAR, SEM, SARMA, CAR, etc. Moreover, it allows one to detect many forms of anisotropy by estimating a small number of parameters.

The paper is organized as follows. Section 2 formally analyses the ABE test, develops a generalization, focuses on the kind of anisotropies that it can detect, and studies its power. Section 3 introduces the new modelling approach and illustrates how the form of anisotropy can be estimated and tested on both regularly and irregularly spaced data. Section 4 illustrates the outcomes of the Monte Carlo simulation experiments performed in order to assess the finite-sample properties of the estimators and the power of the test. Section 5 concludes.

2 The ABE isotropy test

2.1 The original ABE test

Consider the following spatial autoregressive model:

$$\begin{cases} y = \rho W y + X \beta + \varepsilon \\ \varepsilon \sim \mathcal{N}_n(0, \sigma^2 I) \end{cases}, \quad (4)$$

defined on a (regular or irregular) grid \mathcal{G}_n of n cells, where $W \in \mathbb{R}^{n \times n}$ is a spatial weight matrix, $X \in \mathbb{R}^{n \times k}$ is a matrix of k exogenous explanatory variables (which may include a unitary column), $\beta \in \mathbb{R}^k$, $\sigma \in \mathbb{R}^+$, and $\rho \in \mathbb{R}$ is such that $I - \rho W$ is positive definite (Ord 1975).

The ABE test requires that neighbours of each cell of \mathcal{G}_n are divided up into two groups according to a direction described by a straight line with slope $\tan \theta$ passing through the centroid of the reference cell. Formally, this result is achieved by defining two directional matrices W_1 and W_2 as follows:

$$(W_j)_{kh} \equiv \mathbb{1}_{\{(c_h - c_k) \in H_j\}} w_{kh}, \quad j = 1, 2, \quad (5)$$

where w_{kh} is the (k, h) element of W , $c_k, c_h \in \mathbb{R}^2$ are the Cartesian coordinates of the centroids of cells $k, h \in \mathcal{G}_n$, $\mathbb{1}_{\{\cdot\}}$ is the indicator function, and H_1, H_2 are the half-planes generated by the straight line passing through the origin $(0, 0)$ and whose angle with abscissa is θ .

The ABE isotropy test is based on the comparison of the following model

$$\begin{cases} y = (\rho_1 W_1 + \rho_2 W_2)y + X\beta + \varepsilon \\ \varepsilon \sim \mathcal{N}_n(0, \sigma^2 I) \end{cases} \quad (6)$$

to model (4) in terms of goodness of fit, hence the null hypothesis to be tested is $\rho_1 = \rho_2$, since, if the data generating process $\{y_{st}\}$ is isotropic, the spatial dependence (captured by autoregressive parameters ρ_1 and ρ_2) should be the same along any direction.

Note that, from definition (5), the following properties hold:

$$\begin{aligned} W_1 + W_2 &= W, \\ W_1 \odot W_2 &= 0 \in \mathbb{R}^{n \times n}, \end{aligned}$$

where \odot is the Hadamard product (that is, the elementwise matrix product). The first property guarantees that (6) coincides with (4) when the isotropy assumption holds (that is, the models are nested), whereas the latter entails that each neighbour of the cells is assigned (i.e. it has non-zero weight) either to W_1 or to W_2 .

In light of the notation we have introduced in this section, we may formalise Example (1) as follows.

Example 2. Models (2) and (3) can be restated in matrix form as (6) without the regressor matrix X . Define $T_1^h T_2^k y_{st} \equiv y_{s+h, t+k}$, and assume that cells of \mathcal{G}_n are identified according to the matrix indexation.

Model (2) results from $0 < \theta < \pi/2$. In particular, W_1 should include the T_1^{-1} and T_2^{-1} spatial lags, while W_2 should pick T_1 and T_2 out. As explained, in this case the ABE test will not reject the isotropy hypothesis, since both W_1 and W_2 include half spatial lags with coefficient α and half with coefficient β .

On the other hand, model (3) is implied by the condition $-\pi/2 < \theta < 0$. In this case, if we include T_1^{-1} and T_2 in W_1 , and T_2^{-1} and T_1 in W_2 , the ABE test will be able to detect the anisotropy of $\{y_{st}\}$, since W_1 contains only the spatial lags with coefficient α , while W_2 includes the spatial lags with coefficient β . \square

The problems we outlined in Example 1 and 2 are analysed in the framework of a generalized version of the ABE test, where the neighbours are split into $q \geq 2$ groups.

2.2 The q -directional ABE test

Consider a spatial process $\{y_k\}$ defined on a (regular or irregular) two-dimensional grid \mathcal{G}_n with n cells having centroids with Cartesian coordinates $\{c_k\}$ (where $c_k = [c_{k1} \ c_{k2}]^T$). The process is defined as follows:

$$y_k = \sum_{h=1}^n g(k, h, w_{kh}) y_h + \varepsilon_k,$$

where g is a real function, w_{kh} is the (k, h) element of the weight matrix $W \in \mathbb{R}^{n \times n}$, and $\{\varepsilon_k\}$ is an iid spatial process.

We assume that $\{y_k\}$ is homogeneous, thus the function g should depend just on $c_h - c_k$ instead of k and h . Moreover, without loss of generality, we assume

that the weight matrix W incorporates the effect of the Euclidean distance between centroids ($\|c_h - c_k\|_2$). Hence, the resulting model is:

$$y_k = \sum_{h=1}^n f(\theta_{kh}) w_{kh} y_h + \varepsilon_k, \quad (7)$$

where θ_{kh} is the angle of the vector $c_h - c_k$ expressed in polar coordinates. Finally, we assume that $f: \mathbb{R} \rightarrow \mathbb{R}$ is periodic (with period 2π) and it is expandable as a Fourier series. We do not, however, make any assumption about the fundamental period of f , that is, the minimum period of f : we only require that $f(\omega + 2\pi) = f(\omega)$ for any $\omega \in \mathbb{R}$. Hence, there may exist a positive constant $T < 2\pi$ such that $f(\omega + T) = f(\omega)$ for any $\omega \in \mathbb{R}$. Model (7) is isotropic if $f(\theta_{kh})$ is independent of θ_{kh} , that is, if $f(\theta_{kh})$ is constant.

We may generalise the ABE test by dividing the neighbours according to $q \geq 2$ directions. Consider the following Fourier expansion of f :

$$f(\omega) = \sum_{m=0}^{\infty} a_m \cos(m\omega + \varphi_m), \quad (8)$$

and assume that the round angle is divided into $q \geq 2$ equal parts starting from θ . That is, \mathbb{R} is partitioned into intervals having the form $I_r \equiv [\theta + 2\pi(r-1)/q, \theta + 2\pi r/q]$ for $r \in \mathbb{Z}$. We define:

$$\rho_{kh} \equiv \frac{q}{2\pi} \int_{I_{Q(\theta_{kh})}} f(\omega) d\omega, \quad (9)$$

where $Q: \mathbb{R} \rightarrow \mathbb{Z}$ is the function such that $\theta_{hk} \in I_{Q(\theta_{kh})}$, that is, $Q(\theta_{kh})$ gives the value r such that $\theta_{hk} \in I_r$.

By analogy with the basic ABE method, the q -directional version requires the unrestricted model

$$y = \left(\sum_{r=1}^q \rho_r W_r \right) y + \varepsilon \quad (10)$$

to be tested against the restricted model

$$y = \rho \left(\sum_{r=1}^q W_r \right) y + \varepsilon, \quad (11)$$

where ρ_r and W_r ($r = 1, \dots, q$) are the directional parameters and matrices. In particular, $\rho_r \equiv \rho_{kh}$ for every $(k, h) \in \mathcal{G}_n$ such that $r = Q(\theta_{kh})$, while $(W_r)_{kh} \equiv \mathbf{1}_{\{r=Q(\theta_{kh})\}} w_{kh}$. Thus, in this case, the isotropy hypothesis corresponds to the restriction $\rho_1 = \rho_2 = \dots = \rho_q$.

2.3 Factors affecting the power of the ABE test

Rearranging Equations (8) and (9), we obtain:

$$\rho_{kh} = \frac{q}{2\pi} \sum_{m=0}^{\infty} \int_{I_{Q(\theta_{kh})}} a_m \cos(m\omega + \varphi_m) d\omega, \quad (12)$$

and integrating (12) we have:

$$\rho_{kh} = a_0 \cos \varphi_0 + \frac{q}{2\pi} \sum_{m=1}^{\infty} \frac{a_m}{m} \left[\sin(m\omega + \varphi_m) \right]_{\theta+2\pi(Q(\theta_{kh})-1)/q}^{\theta+2\pi Q(\theta_{kh})/q}. \quad (13)$$

As concerns (13), some remarks are in order.

First, the terms of the sum in (13) converge to zero regardless of the value of θ and θ_{kh} as the angular frequency m of the associated harmonic increases. This implies that the power of the ABE test is low in detecting anisotropies originating from high-frequency components of f . As (13) shows, the terms converge to zero because of the factor m^{-1} , hence, given q , high-frequency harmonics of f can be detected only if their amplitudes $|a_m|$ are large enough to counterbalance the effect of m^{-1} .

Second, the power of the ABE test can be increased for both low and high frequency components of f by increasing the number of partitions q of the round angle. This may be appreciated if we note that

$$\sup_{\theta} \left\{ \text{range}_r \left(\left[\sin(m\omega + \varphi_m) \right]_{\theta+2\pi(r-1)/q}^{\theta+2\pi r/q} \right) \right\} \uparrow [-1, 1] \quad (14)$$

as $q \rightarrow \infty$. In fact, when the range in (14) is narrow, the power of the q -directional ABE test in detecting anisotropy originating from the harmonic with angular frequency m is low because the variability of the coefficients ρ_r is small.

Third, the power of the q -directional ABE test is significantly affected by the reference angle θ through harmonics of f whose ratio a_m/m is relatively high, and angular frequency is close to $q/2$. In order to prove this fact, some basics in signal theory are needed (see e.g. Priemer 1991).

A typical problem of signal theory is to reconstruct an analogue signal (i.e. a continuous function of time) from a finite number of observations. Such a task can be easily handled when the signal is periodic, since Fourier analysis allows one to decompose the original signal as a sum of sine and cosine waves (called ‘‘harmonics’’) with various amplitudes, phase, and frequencies. If the observations of the signal are properly collected, it is possible to detect and estimate the main harmonics of the analogue signal and reconstruct it with various levels of accuracy.

The reconstruction of the periodic analogue signal requires it to be observed (sampled) several times throughout its period. As the number of observations per period (the so-called ‘‘sampling frequency’’) increases, the accuracy of the reconstructed signal improves. This principle is formalised by the Nyquist-Shannon theorem (see e.g. Bloomfield 2000), which states that when a periodic signal is sampled at a certain frequency ω , it is possible to identify only its harmonics whose frequency is not higher than $\omega/2$. The critical frequency $\omega/2$ is known as Nyquist frequency.

In terms of the problem about the ABE test, we may consider the function f as an analogue signal which has period 2π and is sampled q times at regular intervals on $[0, 2\pi)$ (hence, the angular sampling frequency is q). The observations resulting from such a sampling scheme are the autoregressive coefficients $\{\rho_1, \dots, \rho_q\}$ of equation (10). In particular, unlike traditional signal sampling, the ρ_r s do not represent point values of f , but are its mean values over intervals of width $2\pi/q$, as equation (9) clearly shows.

The peculiarity of the sampling scheme implied by the q -directional ABE test does not prevent us from considering it as an approximation of the usual signal sampling scheme as q diverges, since $\lim_{q \rightarrow \infty} \rho_{kh} = f(\theta_{kh})$. In light of this, we note that $q/2$ represents the Nyquist frequency, that is the highest-frequency component of f that can be identified.

The reason why only harmonics with angular frequency $m \approx q/2$ have a strong impact on the power of the q -directional ABE test through θ can be understood if we note that harmonics with angular frequency $m \ll q/2$ are identified with precision (there are many observations for each period), and thus a change in θ does not substantially improve their estimates (the range in (14) is not much affected). On the other hand, the impact of θ on ρ_{kh} decreases for harmonics with angular frequency $m \gg q/2$ both because of the coefficient m^{-1} of the terms in (13), and because there is a confounding phenomenon (called aliasing) that prevents from correctly identifying such harmonics (as stated in the Nyquist-Shannon theorem).

To summarise, the power of the q -directional ABE test can be improved by increasing q or by optimizing θ . The first solution has some limitations, since as q gets larger, the number of directional autoregressive parameters $\{\rho_1, \dots, \rho_q\}$ increases, and this results in a loss of degrees of freedom. Moreover, a high number of directional weight matrices W_1, \dots, W_q gives rise to multicollinearity problems among the regressors in (10). Last but not least, processing several $n \times n$ directional matrices may be computationally troublesome.

On the other hand, the optimization of θ is worthwhile when q is small and harmonics to be detected have angular frequencies close to $q/2$. Nevertheless, the optimal reference angle θ^* cannot be easily estimated because it depends on f , which is obviously unknown. This problem may be overcome by performing the q -directional ABE test for several values of θ in order to verify whether anisotropy is detected for some $\theta \in [0, 1/q)$. Although no theoretical reason bars this approach, the construction of many sets of directional matrices (W_1, \dots, W_q) may be computationally demanding.

The problem of finding the optimal values of q and θ is overcome by the isotropy test we propose in Section 3, which may be interpreted as a ∞ -directional ABE test where the reference angle θ is unnecessary, and the coefficients of the Fourier expansion of f are estimated instead of the directional autoregressive parameters ρ_r .

3 A new isotropy test

The problems discussed in the previous section arise from the discretisation of the interval $[0, 2\pi)$ and the consequent need of defining two partitioning parameters (θ and q) and integrating the function f . These drawbacks of the q -directional ABE test are wiped out when $q \rightarrow \infty$.

When $q \rightarrow \infty$, the autoregressive parameters $\{\rho_r\}$ can no longer be estimated because they are infinite. However it is possible to estimate the Fourier expansion of f : although the Fourier coefficients are infinite too, usually just a few of them have to be estimated in order to detect anisotropies. For example, in Fourier analysis the harmonic with angular frequency m is fully identified by only two coefficients, while the q -dimensional ABE test requires $q \geq 2m$, that is, at least $2m$ coefficients should be estimated in order to detect the same harmonic.

A further advantage of the test we are going to develop derives from the orthogonality of harmonics in a Fourier series. This property allows us to improve the accuracy of the approximation of f without increasing the multicollinearity of regressors. This issue distinguishes this test from the q -dimensional ABE test, where multicollinearity grows as q gets larger.

The new testing approach requires to restate (8) as

$$f(\omega) = \rho + \sum_{m=1}^{\infty} [\rho_{cm} \cos(m\omega) + \rho_{sm} \sin(m\omega)], \quad (15)$$

where $\rho \equiv a_0 \cos \varphi_0$, $\rho_{cm} \equiv a_m \cos \varphi_m$, $\rho_{sm} \equiv -a_m \sin \varphi_m$. It follows that (7) can be rewritten as:

$$y_k = \rho \sum_{h=1}^n w_{kh} y_h + \sum_{m=1}^{\infty} \left(\rho_{cm} \sum_{h=1}^n \cos(m\theta_{kh}) w_{kh} y_h + \rho_{sm} \sum_{h=1}^n \sin(m\theta_{kh}) w_{kh} y_h \right) + \varepsilon_k,$$

or, in matrix notation,

$$y = \left(\rho W + \sum_{m=1}^{\infty} [\rho_{cm} A_m \odot W + \rho_{sm} B_m \odot W] \right) y + \varepsilon, \quad (16)$$

where $(A_m)_{kh} = \cos(m\theta_{kh})$, $(B_m)_{kh} = \sin(m\theta_{kh})$. Given the matrix of coordinates of centroids $C \in \mathbb{R}^{n \times 2}$, the angles θ_{kh} can be computed as follows:

$$\theta_{kh} = \arctan2((C_y)_{kh}, (C_x)_{kh}),$$

where:

$$C_x \equiv (C [1 \ 0]^T \iota_n^T)^T - (C [1 \ 0]^T \iota_n^T),$$

$$C_y \equiv (C [0 \ 1]^T \iota_n^T)^T - (C [0 \ 1]^T \iota_n^T),$$

and $\arctan2: \mathbb{R}^2 \rightarrow [-\pi, \pi]$ is the inverse function of \tan .

Model (16) potentially allows one to model, estimate, and test any form of anisotropy based on any real function $f: \mathbb{R} \rightarrow \mathbb{R}$ of period 2π expandable in a Fourier series. The isotropy condition is:

$$\rho_{c1} = \rho_{c2} = \dots = \rho_{s1} = \rho_{s2} = \dots = 0, \quad (17)$$

that is, (16) is isotropic when f has no harmonic components, so that it is constant. If, in addition to (17), we require that $\rho = 0$, we can test the hypothesis of no spatial correlation.

As mentioned above, only a finite number of harmonics can be estimated and tested, and this implies that only some terms of the sum in (16) can be included into the model to be fitted. Nonetheless, a very small number of harmonics can provide an accurate approximation of the functions f relevant for applications, as the high-frequency components of f have a marginal role in defining the form of anisotropy in econometric analysis. The following example considers a commonly encountered anisotropy structure.

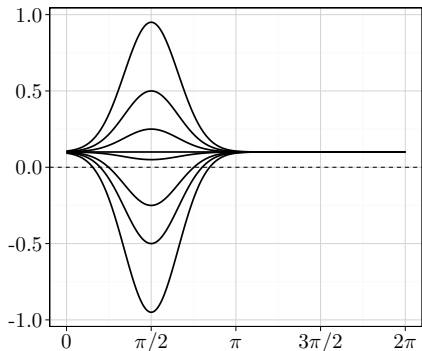


Figure 1: Function (18) for $\kappa = \pi/2$ and various values of α (from top to bottom): 0.85, 0.4, 0.15, 0, -0.05 , -0.35 , -0.6 , -1.05 .

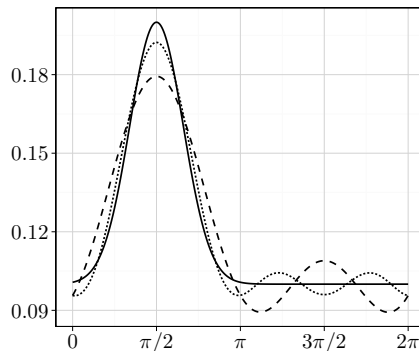


Figure 2: Function (18) with $\kappa = \pi/2$ and $\alpha = 0.1$ (solid line) and its Fourier series truncated at the second term (dashed line) and at the third term (dotted line).

Example 3. The function

$$f(\omega) = 0.1 + \alpha e^{-2(\omega - \kappa)^2}, \quad (18)$$

plotted in Figure 1 for various values of α and $\kappa = \pi/2$ may be suitable for describing the North-South asymmetries existing among regions or administrative units in a country.

As Figure 1 shows, (18) with $\kappa = \pi/2$ defines a spatial dependence uniform in all directions except for the North ($\omega = \pi/2$): as ω gets closer to $\pi/2$, the spatial dependence becomes stronger (when $\alpha > 0$), weaker ($-0.1 < \alpha < 0$), or negative ($\alpha < -0.1$). The parameters α and κ respectively determine the strength and the direction of the anisotropy.

Figure 2 shows the Fourier expansions of f for $\alpha = 0.1$ truncated at the second and third term. The function is reasonably well approximated by a Fourier expansion truncated at the second term. The reason why this happens is related to the Fourier coefficients of f displayed in Figure 3. Figure 3 shows that the first two harmonics explain most of the variability of f , and only a negligible improvement is achieved by including also the third or fourth harmonic.

Figure 4 reports the Fourier coefficients of the step function:

$$f(\omega) = 0.1 + 0.1 \cdot \mathbf{1}_{\{\omega \in (\pi/4, 3\pi/4)\}}, \quad (19)$$

whose shape is rather different from (18) with $\kappa = \pi/2$. It is worth noting that also in this case the first two/three harmonics explain most of the variability of (19). \square

The harmonics of f may be given a precise interpretation in terms of the shape of the anisotropy of a process, especially when there are few components. In general, the harmonic with angular frequency m describes a spatial dependence stronger (or weaker) along m directions equally spaced on the round angle.

Consider, for example, the harmonic $-\cos 2\omega$ illustrated in Figure 5a. In this case the harmonic describes a positive and symmetric spatial dependence along the direction identified by angles $\pi/2$ (North) and $3\pi/2$ (South), and a negative

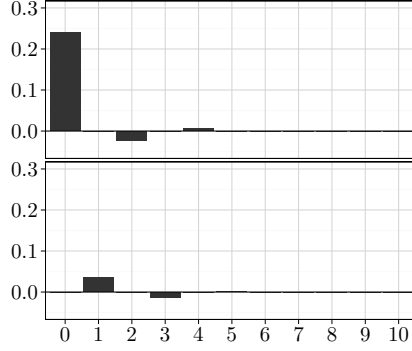


Figure 3: Fourier coefficients $\rho, \rho_{c1}, \dots, \rho_{c10}$ (upper panel) and $\rho_{s1}, \dots, \rho_{s10}$ (lower panel) of function (18) for $\kappa = \pi/2$ and $\alpha = 0.1$.

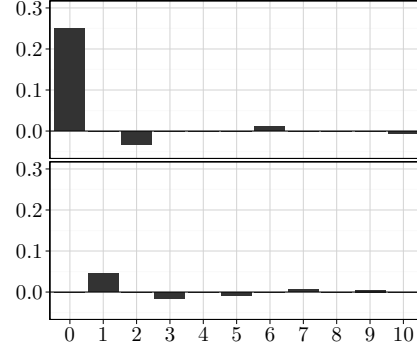
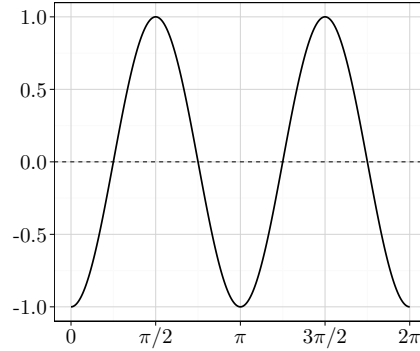
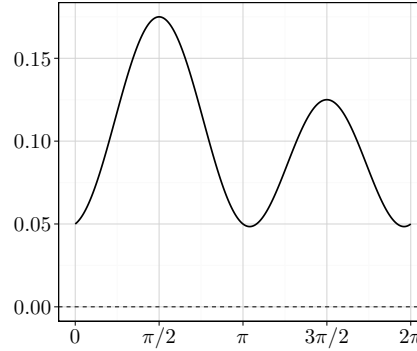


Figure 4: Fourier coefficients $\rho, \rho_{c1}, \dots, \rho_{c10}$ (upper panel) and $\rho_{s1}, \dots, \rho_{s10}$ (lower panel) of function (19).



(a) $f(\omega) = -\cos 2\omega$.



(b) $f(\omega) = 0.1 + 0.025 \sin \omega - 0.05 \cos 2\omega$.

Figure 5: The f functions associated to a single harmonic (Figure 5a), and to a superposition of two harmonics with angular frequencies $m = 1$ and $m = 2$ (Figure 5b).

spatial dependence along direction 0 (East) and π (West). In other words, the effect of the harmonic $-\cos 2\omega$ consists in (symmetrically) increasing the positive spatial dependence along the North-South direction, and decreasing (or making negative) the spatial dependence along the West-East direction. Obviously, the overall form of the anisotropy depends also on the other harmonics of f , the constant term and their relative amplitudes.

It is possible to describe a relevant class of anisotropies by means of only one or two harmonics, as hinted in Example 3. Figure 5b displays the function

$$f(\omega) = 0.1 + 0.025 \sin \omega - 0.05 \cos 2\omega,$$

which consists of two harmonics (with angular frequencies $m = 1$ and $m = 2$ respectively) and a constant term. As Figure 5b shows, spatial dependence is weak along the West-East direction ($\omega \approx 0$ and $\omega \approx \pi$), while it gets stronger and asymmetric along the North-South direction ($\omega \approx \pi/2$ and $\omega \approx 3\pi/2$). This shape of f may be useful for describing a spatial dependence that is both stronger

(or weaker) and asymmetric along one direction.

The specification of model (16) requires some adaptations when observations are regularly spaced. In fact, when the data come from regular lattices or other regular structures, the set of values taken by θ_{kh} is regularly spaced too, and some components of f may be redundant or undersampled (i.e. there is aliasing). If these components of f are not removed, the model is not identifiable from a statistical point of view.

Consider, for example, a rectangular grid \mathcal{G}_n . We have $\theta_{kh} \in \{0, \pi/2, \pi, 3\pi/2\}$ for all $\theta_{kh} \in \mathcal{G}_n$, hence the angular sampling frequency is 4. In this case, according to the Nyquist-Shannon theorem, only harmonics with angular frequency 1 and 2 should be considered. Moreover, the component $\sin 2\omega$ is useless, since $\sin 2\theta_{kh} = 0$ for any $(k, h) \in \mathcal{G}_n$. Thus, the symmetric anisotropies are captured only by $\cos 2\omega$, while asymmetries originate from $\sin \omega$ (along the North-South direction) and $\cos \omega$ (along the East-West direction). Hence, (16) becomes:

$$y = (\rho W + \rho_{c1} A_1 \odot W + \rho_{s1} B_1 \odot W + \rho_{c2} A_2 \odot W) y + \varepsilon.$$

The test illustrated in this section can be applied to hypotheses different from (17). As mentioned above, the restriction $\rho = 0$ along with (17) defines the hypothesis of no spatial correlation. It is worth noting that a test based on these two restrictions may be more powerful in detecting spatial dependence than a test for restriction $\rho = 0$ alone. This happens whenever f has form (15) with $\rho = 0$ and some ρ_{cm} or ρ_{sm} different from zero.

In some cases, it may be necessary to test for the presence of a specific form of anisotropy or the presence of asymmetries or specific directions in f . Such kind of hypotheses can be easily translated in terms of restrictions on the coefficients of the Fourier expansion of f and tested like any other parameter restriction.

Testing specific forms of anisotropy may be interesting in itself, or when the data generating process have to be consistent with certain properties in order to perform further analyses or to apply some estimation techniques. This is the case, for example, of unilateral approximation (Arbia et al. 2014), which can be used for fitting spatial models defined on a rectangular lattice only if the underlying process is symmetric.

It is worth noting that the possibility of testing specific forms of anisotropy represents a strong advantage of this testing approach with respect to other isotropy tests such as the q -directional ABE test or the test suggested by Molina and Feito (2002) which is implicitly based on a specification of (16) truncated at the first term (that is, only the fundamental harmonic with unit angular frequency and the constant term are considered).

In this section, the model used as a reference is (4), which is referred to as SAR in the spatial econometric literature (see e.g. LeSage and Pace 2009). However, our testing approach can be easily adapted to other econometric models for areal data like SEM, Durbin, MESS (see e.g., LeSage and Pace 2009; Arbia 2014), CAR (see e.g. Wall 2004; Cressie 1993), and models based on multiple weight matrices like SAC and SARMA (LeSage and Pace 2009).

4 Simulation Study

In order to study the power of the test in finite samples, we perform two Monte Carlo simulation experiments on regular and irregular grids.

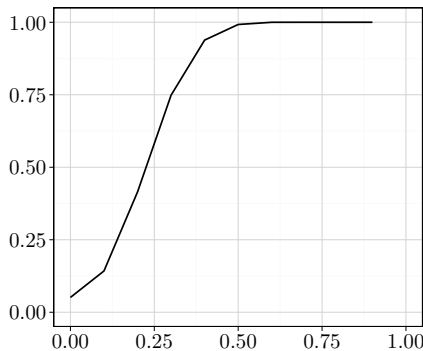


Figure 6: Empirical power of the isotropy test for model (20) as a function of $|\rho_1 - \rho_2|$. Complete results are displayed in Table 1.

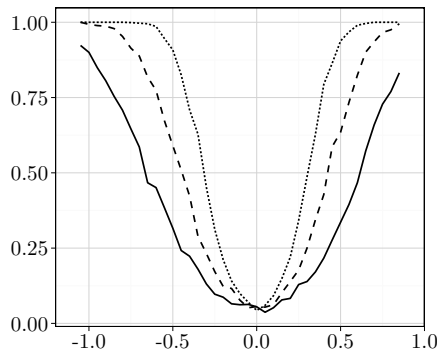


Figure 7: Empirical power of the isotropy test on the irregular grid as a function of α , with $n = 400$, $v = 2$, and $\sigma^2 = 1$ (solid line), $\sigma^2 = 1/2$ (dashed line), and $\sigma^2 = 1/4$ (dotted line). Complete results are displayed in Table 2.

We have considered a spatial process on a 20×20 rectangular lattice defined as follows:

$$\begin{cases} y = (\rho_1 W_1 + \rho_2 W_2)y + X\beta + u \\ u \sim \mathcal{N}_n(0, \sigma^2 I) \end{cases}, \quad (20)$$

where $y \in \mathbb{R}^n$, $X \in \mathbb{R}^n$, $\beta = 1$, $\sigma^2 = 1$, $n = 400$. The directional weight matrices W_1 and W_2 are defined as $W_1 \equiv C_1 \odot W$ and $W_2 \equiv C_2 \odot W$, where $C_1 \in \{0, 1\}^{n \times n}$ and $C_2 \in \{0, 1\}^{n \times n}$ are the contiguity matrices of neighbours along the vertical and horizontal direction respectively. The matrix $W \in \mathbb{R}^{n \times n}$ results from a row-standardization of a weight matrix based on the rook neighbourhood rule, and its non-zero elements are independently drawn from the beta distribution $B(2, 0.8)$. The regressor X consists of a column of values drawn from the standard normal distribution.

We consider several values of ρ_1 and ρ_2 (see Table 1). For each pair (ρ_1, ρ_2) we simulate 1000 models and test the isotropy hypothesis ($\rho_1 = \rho_2$). All the models share the same directional weight matrices (W_1 and W_2) and the same regressor X .

The unrestricted model is based on $f(\omega) = \rho + \rho_{c2} \cos(2\omega)$, so that the fitted model is:

$$y = \rho W y + \rho_{c2} (A_2 \odot W) y + X\beta + \varepsilon.$$

The isotropy hypothesis ($\rho_{c2} = 0$) is tested by means of the likelihood ratio test at a significance level of 5%. Complete results are shown in Table 1, while Figure 6 summarises the empirical power as a function of $|\rho_1 - \rho_2|$.

As Figure 6 clearly shows, the power of the new test sharply increases as the absolute difference between ρ_1 and ρ_2 exceeds 0.1, and it basically equals 1 when $|\rho_1 - \rho_2|$ is larger than 0.50.

The irregular grid Monte Carlo simulations are based on data generating process (7) with a vector of regressor coefficients $\beta = \iota_2$, and a regressor matrix $X = [\iota_n, X_1] \in \mathbb{R}^{n \times 2}$ where X_1 is a vector of standard normal random variables. The grid \mathcal{G}_n consists of the unit square $[0, 1]^2$ split into 400 irregular convex

	-0.90	-0.80	-0.70	-0.60	-0.50	-0.40	-0.30	-0.20	-0.10	0.00
-0.90	—	—	—	—	—	—	—	—	—	1.000
-0.80	—	—	—	—	—	—	—	—	1.000	1.000
-0.70	—	—	—	—	—	—	—	0.993	1.000	1.000
-0.60	—	—	—	—	—	—	0.766	0.943	0.995	1.000
-0.50	—	—	—	—	—	0.157	0.436	0.725	0.947	0.990
-0.40	—	—	—	—	0.154	0.064	0.126	0.404	0.726	0.939
-0.30	—	—	—	0.773	0.429	0.139	0.054	0.153	0.428	0.754
-0.20	—	—	0.992	0.945	0.752	0.422	0.141	0.042	0.140	0.417
-0.10	—	1.000	1.000	0.993	0.950	0.751	0.414	0.139	0.051	0.148
0.00	1.000	0.999	1.000	1.000	0.991	0.933	0.751	0.392	0.144	0.035
0.10	—	1.000	1.000	1.000	1.000	0.991	0.913	0.727	0.402	0.142
0.20	—	—	1.000	1.000	1.000	1.000	0.997	0.943	0.764	0.412
0.30	—	—	—	1.000	1.000	1.000	0.999	0.988	0.927	0.750
0.40	—	—	—	—	1.000	1.000	1.000	1.000	0.995	0.943
0.50	—	—	—	—	—	1.000	1.000	1.000	1.000	0.995
0.60	—	—	—	—	—	—	1.000	1.000	1.000	1.000
0.70	—	—	—	—	—	—	—	1.000	1.000	1.000
0.80	—	—	—	—	—	—	—	—	1.000	1.000
0.90	—	—	—	—	—	—	—	—	—	1.000

	0.10	0.20	0.30	0.40	0.50	0.60	0.70	0.80	0.90
-0.90	—	—	—	—	—	—	—	—	—
-0.80	1.000	—	—	—	—	—	—	—	—
-0.70	1.000	1.000	—	—	—	—	—	—	—
-0.60	1.000	1.000	1.000	—	—	—	—	—	—
-0.50	1.000	1.000	1.000	1.000	—	—	—	—	—
-0.40	0.987	1.000	1.000	1.000	1.000	—	—	—	—
-0.30	0.943	0.992	1.000	1.000	1.000	1.000	—	—	—
-0.20	0.748	0.921	0.989	0.999	1.000	1.000	1.000	—	—
-0.10	0.400	0.725	0.938	0.995	1.000	1.000	1.000	1.000	—
0.00	0.113	0.408	0.732	0.936	0.992	1.000	1.000	1.000	1.000
0.10	0.060	0.148	0.423	0.748	0.941	0.995	1.000	1.000	—
0.20	0.127	0.045	0.143	0.436	0.740	0.958	0.991	—	—
0.30	0.396	0.152	0.057	0.139	0.403	0.739	—	—	—
0.40	0.746	0.416	0.162	0.052	0.149	—	—	—	—
0.50	0.935	0.759	0.429	0.131	—	—	—	—	—
0.60	0.991	0.939	0.795	—	—	—	—	—	—
0.70	1.000	0.995	—	—	—	—	—	—	—
0.80	1.000	—	—	—	—	—	—	—	—
0.90	—	—	—	—	—	—	—	—	—

Table 1: Empirical evaluation of the power of the isotropy test on model (20) for various values of ρ_1 (columns) and ρ_2 (rows). The evaluation of the empirical power is based on 1000 simulations for each couple (ρ_1, ρ_2) . The coefficient restriction has been tested by means of the likelihood ratio test with a 5% significance level.

polygons obtained by means of a Voronoi tessellation generated by 400 points drawn from the uniform distribution on $[0, 1]^2$. The weight matrix W results from row-standardization of a weight matrix \bar{W} built according to the contiguity criterion, and whose non-zero elements equal the area of the neighbouring cell. That is, the (k, h) element of \bar{W} is defined as:

$$(\bar{W})_{kh} \equiv \begin{cases} A_h & \text{if } h \text{ is a neighbour of } k \\ 0 & \text{otherwise} \end{cases},$$

where A_h is the area of cell h .

The function f is of type (18), and the simulation has been performed for several values of α , provided that the invertibility condition is satisfied, that is $|f(\omega)| < 1$ for any $\omega \in [0, 2\pi)$.

The unrestricted models include either the first two ($v = 2$) or the first three ($v = 3$) harmonics. The innovation $\{\varepsilon_{st}\}$ is an iid Gaussian process with

variance $\sigma^2 = 1, 1/2, 1/4$. For each value of α , σ^2 and v , 1000 models have been simulated, fitted, and tested by means of the likelihood ratio test, with a significance level equal to 5%. All the models with the same α , σ^2 and v share the matrix of regressors X and the weight matrix W . The grid \mathcal{G}_n is shared too.

In addition to the experiments just described, we have also performed a simulation on an irregular grid with $n = 800$ cells. This simulation has been structured like the previous one with $v = 2$ and $\sigma^2 = 1$, except for the number of replications, equal to 300 instead of 1000.

Table 2 reports the complete results, while Figure 7 displays the power of the test as a function of α for models where $v = 2$ and $n = 400$. According to Table 2, there are no benefits from including the third harmonics, which indeed seems, in many cases, to reduce the power of the test, although the difference is not statistically significant at the 5% level. This result is consistent with Figure 3, according to which the first two harmonics (along with the constant term) can explain most of the variation of f .

Figure 7 shows that the power of the test is rather sensitive to the variance of the innovation process. Moreover, we note that the power function in the case with $n = 800$ and $\sigma^2 = 1$ is not statistically different (again at the 5% level) from the case with $n = 400$ and $\sigma^2 = 1/2$.

Finally, it is worth highlighting that in both the lattice and the irregular grid model a sharp increase of the power of the test is observed when the number of regressors is larger.

5 Conclusion

The modelling approach proposed in this paper allows one both to estimate and test the form of the anisotropy of a spatial process. The semi-parametric nature of this method makes it applicable to various models for areal data based on weight matrices, while the algebraic properties of the Fourier series minimise the multicollinearity problems which may be originated by an accurate specification of the anisotropy function f .

The test relies on the assumption of homogeneity of the data generating process, and this may be, in some cases, a rather strong assumption. The generalisation of the test to non-homogeneous spatial processes is a subject that deserves further research.

References

- Arbia, G. (2014). *A Primer for Spatial Econometrics*. Palgrave.
- Arbia, G., M. Bee and G. Espa (2013). ‘Testing Isotropy in Spatial Econometric Models’. In: *Spatial Economic Analysis* 8.3, pp. 228–240.
- Arbia, G., M. Bee, G. Espa and F. Santi (2014). *Fitting Spatial Econometric Models through the Unilateral Approximation*. Discussion Paper 8. Department of Economics and Management, University of Trento.
- Bloomfield, P. (2000). *Fourier Analysis of Time Series*. 2nd ed. John Wiley & Sons.
- Cabaña, E. M. (1987). ‘Affine Processes: A Test of Isotropy Based on Level Sets’. In: *SIAM Journal on Applied Mathematics* 47.4, pp. 886–891.

α	$v = 2$ $\sigma^2 = 1$ $n = 400$	$v = 3$ $\sigma^2 = 1$ $n = 400$	$v = 2$ $\sigma^2 = 1/2$ $n = 400$	$v = 3$ $\sigma^2 = 1/2$ $n = 400$	$v = 2$ $\sigma^2 = 1/4$ $n = 400$	$v = 3$ $\sigma^2 = 1/4$ $n = 400$	$v = 2$ $\sigma^2 = 1$ $n = 800$
-1.05	0.923	0.888	1.000	0.997	1.000	1.000	1.000
-1.00	0.900	0.870	0.993	0.992	1.000	1.000	1.000
-0.95	0.849	0.817	0.989	0.997	1.000	1.000	0.997
-0.90	0.806	0.771	0.987	0.981	1.000	1.000	0.997
-0.85	0.754	0.735	0.979	0.961	1.000	1.000	0.970
-0.80	0.708	0.642	0.953	0.945	1.000	1.000	0.957
-0.75	0.646	0.605	0.914	0.933	0.999	0.999	0.930
-0.70	0.586	0.540	0.888	0.866	0.997	0.993	0.907
-0.65	0.467	0.469	0.818	0.816	0.995	0.991	0.820
-0.60	0.451	0.435	0.774	0.746	0.986	0.975	0.783
-0.55	0.384	0.347	0.673	0.640	0.946	0.948	0.727
-0.50	0.316	0.266	0.590	0.550	0.908	0.888	0.583
-0.45	0.242	0.221	0.509	0.438	0.825	0.808	0.500
-0.40	0.223	0.188	0.423	0.381	0.709	0.722	0.427
-0.35	0.180	0.155	0.289	0.286	0.628	0.579	0.297
-0.30	0.131	0.115	0.232	0.192	0.452	0.424	0.230
-0.25	0.097	0.088	0.172	0.161	0.312	0.304	0.143
-0.20	0.087	0.090	0.123	0.120	0.212	0.188	0.110
-0.15	0.065	0.073	0.116	0.080	0.141	0.124	0.087
-0.10	0.062	0.064	0.077	0.066	0.099	0.073	0.067
-0.05	0.063	0.055	0.052	0.061	0.070	0.058	0.057
0.00	0.055	0.069	0.056	0.046	0.043	0.047	0.063
0.05	0.037	0.065	0.054	0.046	0.060	0.074	0.067
0.10	0.052	0.068	0.062	0.074	0.092	0.082	0.060
0.15	0.078	0.069	0.102	0.092	0.149	0.121	0.087
0.20	0.083	0.083	0.139	0.121	0.220	0.206	0.147
0.25	0.129	0.112	0.177	0.171	0.342	0.334	0.157
0.30	0.139	0.128	0.250	0.222	0.487	0.453	0.243
0.35	0.171	0.181	0.344	0.330	0.628	0.607	0.280
0.40	0.217	0.207	0.428	0.380	0.794	0.760	0.487
0.45	0.277	0.275	0.587	0.526	0.864	0.860	0.537
0.50	0.336	0.312	0.635	0.657	0.938	0.941	0.657
0.55	0.395	0.372	0.734	0.716	0.968	0.978	0.730
0.60	0.467	0.451	0.824	0.804	0.990	0.986	0.800
0.65	0.573	0.535	0.901	0.888	0.996	1.000	0.893
0.70	0.659	0.600	0.935	0.927	1.000	1.000	0.923
0.75	0.728	0.690	0.966	0.969	1.000	1.000	0.960
0.80	0.770	0.767	0.975	0.989	1.000	1.000	0.990
0.85	0.832	0.818	0.995	0.991	1.000	1.000	0.990

Table 2: Empirical evaluation of the power of the isotropy test for model (7) based on function (18) with $\kappa = \pi/2$ for various values of α , σ^2 , n , and v . The number of replications used for evaluating the empirical power is 1000 for all models where $n = 400$, and 300 for the single model with $n = 800$. The coefficient restriction has been tested by means of the likelihood ratio test with a 5% significance level.

- Cressie, N. A. C. (1993). *Statistics for Spatial Data*. John Wiley & Sons.
- Guan, Y., M. Sherman and J. A. Calvin (2004). ‘A Nonparametric Test for Spatial Isotropy Using Subsampling’. In: *Journal of the American Statistical Association* 99.467, pp. 810–821.
- LeSage, J. P. and R. K. Pace (2009). *Introduction to Spatial Econometrics*. Chapman&Hall.
- Molina, A. and F. R. Feito (2002). ‘A method for testing anisotropy and quantifying its direction in digital images’. In: *Computer & Graphics* 26, pp. 771–784.
- Ord, J. K. (1975). ‘Estimation Methods for Models of Spatial Interaction’. In: *Journal of the American Statistical Association* 70.349, pp. 120–126.
- Priemer, R. (1991). *Introductory Signal Processing*. World Scientific Publishing.
- Ripley, B. D. (1981). *Spatial Statistics*. John Wiley & Sons.

- Wall, M. M. (2004). 'A close look at the spatial structure implied by the CAR and SAR models'. In: *Journal of Statistical Planning and Inference* 121, pp. 311–324.